Multiple neuromodulatory systems activated by acquiring conditioned taste aversion in alert rats revealed by positron emission tomography

Satomi Kobayashi

Nihon University Graduate School of Dentistry,

Major in Pharmacology

(Directors: Prof. Masayuki Kobayashi)

Index

This thesis is based on the following article and the additional results in terms of taste habituation (Fig. 5).

Kobayashi S, Kajiwara M, Cui Y, Sako T, Sasabe T, Hayashinaka E, Wada Y, Kobayashi M (2024) Activation of multiple neuromodulatory systems in alert rats acquiring conditioned taste aversion revealed by positron emission tomography. Brain Res 1822, 148617. (in press)

Abstract

Conditioned taste aversion (CTA) is an essential ability for animals to consume food safely and is regulated by neuromodulatory systems including the dopamine, noradrenaline, serotonin, and acetylcholine systems. However, because few studies focused on a comprehensive understanding of whole-brain activities, how these neuromodulators contribute to the process of CTA remains an open issue. ^{18}F-fluorodeoxyglucose (FDG)-positron emission tomography (PET) can visualize activated regions within the whole brain simultaneously and noninvasively. This study aimed to understand the mechanisms of CTA, especially focusing on the retrieval process after CTA acquisition by FDG-PET imaging. CTA was established in rats that received an intraoral application of saccharin solution (IOAS) on the first day (Day1), a LiCl i.p. injection after an IOAS on Day2, and an IOAS on Day3 (CTA group). The subtraction images of Day3 of the SHAM group, which received a 0.9% NaCl (saline) injection instead of a LiCl on Day2, from those of Day3 of the CTA group revealed increases in FDG signals in multiple brain regions including the substantia nigra, ventral tegmental area, locus coeruleus, dorsal raphe, and nucleus basalis magnocellularis, in addition to the hippocampus and nociception-related regions, including the parabrachial nucleus and solitary nucleus. On the other hand, the visceral pain induced by the LiCl injection increased FDG signals in the primary and secondary somatosensory and insular cortices in addition to the parabrachial nucleus and solitary nucleus. These results suggest that the retrieval process of CTA induces brain regions producing neuromodulators and pain-related brainstem.

Introduction

Conditioned taste aversion (CTA) is a behavior of animals to avoid a particular taste that is followed by an unpleasant ingestion experience, e.g., abdominal pain, nausea, and/or vomiting, and is one of the most important biological defense mechanisms for survival. CTA consists of several processes including acquisition, retrieval, and extinction (Miranda, Ferreira, Ramirez-Lugo, & Bermudez-Rattoni, 2003; Miranda et al., 2017; Yamamoto, Nagai, Shimura, & Yasoshima, 1998), and variable brain regions are involved in the information processing of CTA, which are principally regulated by excitatory glutamatergic and inhibitory gamma-aminobutyric acid (GABA)ergic synaptic transmissions (Ishitobi et al., 2009; Yamamoto, Nagai, Shimura, & Yasoshima, 1998).

In addition to glutamate and GABA, acetylcholine, noradrenaline, serotonin, and dopamine, which are classified as neuromodulators in the central nervous system, contribute to CTA (Likhtik & Johansen, 2019; Miranda, Ferreira, Ramirez-Lugo, & Bermudez-Rattoni, 2003; Yamamoto, Nagai, Shimura, & Yasoshima, 1998). Electrical or chemical lesions of cholinergic (Lopez-Garcia, Fernandez-Ruiz, Escobar, Bermudez-Rattoni, & Tapia, 1993), noradrenergic (Dunn & Everitt, 1987), serotonergic (Lorden & Margules, 1977; Limebeer, Parker, & Fletcher, 2004), and dopaminergic neurons or fibers (Berridge & Robinson, 1998) impare CTA profiles. Notably, CTA profiles are also affected by pharmacological manipulation of these receptors in various brain regions, e.g., muscarinic receptors (Ramirez-Lugo, Miranda, Escobar, Espinosa, & Bermudez-Rattoni, 2003), adrenoceptors (Miranda, LaLumiere, Buen, Bermudez-Rattoni, & McGaugh, 2003; Fukabori et al., 2020; Ishitobi et

al., 2009), 5-HT_{1A} (Wegener, Smith, & Rosenberg, 1997), 5-HT_3 (Tuerke, Limebeer, Fletcher, & Parker, 2012), and dopaminergic receptors (Asin & Montana, 1989; Fenu, Bassareo, & Di Chiara, 2001; Mediavilla, Mahia, Bernal, & Puerto, 2012). Furthermore, during the series of CTA processes, changes in the release amount of neuromodulators are observed: acetylcholine in the insular cortex (IC; Miranda & Bermudez-Rattoni, 1999), noradrenaline in the amygdala (Guzman-Ramos, Osorio-Gomez, Moreno-Castilla, & Bermudez-Rattoni, 2012), serotonin in the hypothalamus but not in the hippocampus (West, Mark, & Hoebel, 1991), and dopamine in the nucleus accumbens (NAc; Mark, Blander, & Hoebel, 1991) and IC (Osorio-Gomez, Guzman-Ramos, & Bermudez-Rattoni, 2017). Although abundant knowledge in terms of the relation between CTA and neuromodulators has been accumulated, few studies have focused on a comprehensive understanding of brain-wide activities: each CTA process is regulated uniquely by each neuromodulator in a distinct brain region.

Positron emission tomography (PET) and functional magnetic resonance imaging (fMRI) are noninvasive functional brain imaging techniques that provide a global overview of neural activities and enable us to scan the same animals multiple times. The spatial resolution of this imaging technique has improved, and it is now possible to image the brains of rodents. Although the spatiotemporal resolution of fMRI is superior to that of PET, PET has an advantage in imaging the rat brain during sensory stimulation. Especially ^{18}F-fluorodeoxyglucose (FDG), one of the radiolabeled substances for activity mapping of PET, affords high temporal flexibility and allows us to survey neural activities for 30 min or more because FDG is taken up by active regions and remains within the system for at least 1 hr

(Schiffer, Mirrione, & Dewey, 2007). This feature makes it possible to detect activated brain regions during free-moving feeding behaviors without fixation of the head that may disturb intrinsic information processing in the central nervous system (Kobayashi et al., 2013). Because CTA is accompanied by specific disgust behaviors including grooming, tongue protrusion, and gnawing (Grill & Norgren, 1978; Meachum & Bernstein, 1992), FDG-PET has a large advantage when imaging brain-wide activities under physiological conditions.

Utilizing the abovementioned advantages of FDG-PET, the present study aimed to visualize the activated brain regions in response to the retrieval of CTA and examine whether and how the nuclei producing neuromodulators are activated by scanning the whole brain image in alert rats.

Materials and Methods

The rats were maintained and handled in accordance with the National Institutes of Health Guide for the Care and Use of Laboratory Animals. The Institutional Animal Care and Use Committee at Nihon University and RIKEN approved the study protocol.

1. Animals and surgery

In this PET study, we used Wistar rats (male, n = 36) weighing between 200 g and 250 g. Under pentobarbital anesthesia (40-60 mg/kg), an intraoral cannula (PE-10) was unilaterally implanted for oral fluid application. The intraoral cannula was inserted from the mouth lateral to the first maxillary molar, as previously described (Grill & Norgren, 1978; Inui, Yamamoto, & Shimura, 2009; Kobayashi et al., 2013). After surgery, antibiotics (azithromycin hydrate, Pfizer, Tokyo, Japan) were i.p. administered (50 mg/kg). The animals were habituated to saccharin during the recovery period.

2. Gustatory stimulation and PET scanning

One week after surgery, tail vein cannulation was performed under anesthesia with a mixture of 1.5% isoflurane and nitrous oxide/oxygen (7:3). After more than an hour of recovery, FDG (70-75 MBq/0.4 ml) was injected via the cannula under a freely locomotive condition. They also received an intraoral application of 5 mM saccharin solution (IOAS; 0.5 ml/min, 5 min) via the intraoral cannula using a syringe pump (TE-331S, Terumo, Tokyo,

Japan). To avoid adaptation to the gustatory stimulation, the IOAS were repeated three times at 10 min intervals.

Our previous report described the method for PET scanning in detail (Kobayashi et al., 2013), and therefore, only a brief account of the method will be given here. Rats anesthetized with a mixture of 1.5% isoflurane and nitrous oxide/oxygen (7:3) were fixed in the gantry of the PET scanner (microPET Focus 220, Siemens, Knoxville, TN, USA) 45 min after FDG injection. After setting a thermocouple probe and heat blanket, a 30-min emission scan was performed. We acquired emission data by the list mode. We sorted the data into a single sinogram and then reconstructed the data by standard 2D filtered back projection (FBP) with a Ramp filter. A cutoff frequency were set at 0.5 cycles per pixel. Otherwise, the data were reconstructed by a statistical maximum a posteriori probability algorithm (MAP) with 12 iterations with a point spread function effect. We used FBP reconstructed images for quantification and statistical analysis.

3. Experimental groups

The rats that received PET imaging were divided into 5 groups (Fig. 1). The first group, the SHAM group, was scanned just after the IOAS on the first day (Day1, n = 14) and on Day3 (n = 16). On Day2, the SHAM group received an i.p. injection of 0.9% NaCl (saline) with a 2% body weight dose in combination with the IOAS. The second group, the CTA group, was scanned just after the IOAS on Day1 (n = 11) and received 0.14 M LiCl injection with a 2% body weight dose in combination with the IOAS on Day2. On Day3, PET scanning was performed just after the IOAS (n = 11). The third (LiCl group, n = 11) and fourth groups

(NaCl group, n = 7) were scanned just after the i.p. injection of LiCl and saline on Day1, respectively. The fifth group, the IOAS group (n = 10), was scanned just after the IOAS on Day1 and Day3. We excluded the scans with head moving.

4. Image analysis

Individual MAP reconstructed FDG images were coregistered to an FDG template image by use of a mutual information algorithm with Powell's convergence optimization method, implemented with the PMOD software package (version 3.0, PMOD Technologies, Zurich, Switzerland) to perform the voxel-based statistical analysis. The FDG template image was made from 10 age-matched satellite rats prior to the experiment, according to the methods described in Schweinhardt et al., (2003), with slight modification. The FDG template was transformed into the space of an MRI reference template in the stereotactic space (Paxinos & Watson, 2007). The transformation parameters to transform individual MAP images to the FDG template were applied to each FBP reconstructed FDG image. The voxel size of the template was scaled by a factor of 10 to bring it closer to the human brain size: the final voxel size was resampled at 1.2 × 1.2 × 1.2 mm. For the enhancement of statistical power, an isotropic Gaussian kernel (6-mm full width at half maximum) spatially smoothed to each FBP image.

SPM8 software was used for voxel-based statistical analyses. To detect significant differences between treatment groups, we used a two-sample *t*-test. Global uptake differences between individual FDG scans were count normalized to the whole-brain uptake. We set the statistical threshold at $P < 0.005$ or $P < 0.001$ (uncorrected) accompanying an extent

threshold of 150 contiguous voxels. To define the voxels showing significant differences by experimental condition, *T*-value maps of the results were overlaid on the MRI template.

Results

1. Behaviors

In this study, we applied conditioned stimuli (CS) and unconditioned stimuli (US) to the free-moving rats, which induced various behaviors, as previously reported (Grill & Norgren, 1978; Meachum & Bernstein, 1992). The intraoral application of saccharin solution (IOAS) via the cannula, the CS, mostly induced behaviors such as grooming and licking without disgust behaviors. The i.p. injection of LiCl as the US frequently induced pain-related behaviors including writhing syndrome and freezing, whereas the i.p. injection of saline did not show such behaviors. Furthermore, we observed rats in which CTA was established by coapplication of the IOAS and i.p. injection of LiCl. They did not lick the saccharin solution but showed several aversive behaviors such as gaping, freezing, and digging.

2. Subtraction of Day3 saccharin intake in the SHAM group from the CTA group

In the first PET imaging experiment, Day3 PET images of the SHAM group were subtracted from the Day3 images of the CTA group, which provides the difference in the responses to the IOAS between rats with and without CTA (Fig. 2).

The CTA group showed a positive difference in the uptake of FDG in the solitary nucleus (Sol; Fig. 2C). Additionally, the ventromedial thalamic nucleus and zona incerta in the thalamus (Fig. 2B), nucleus basalis magnocellularis (NBM; Fig. 2D), substantia nigra (Fig. 2E) in the basal ganglia, posterior thalamic nuclear group (Fig. 2E), and parasubiculum

(PaS; Fig. 2H) in the limbic system showed larger increases in FDG uptake in the CTA group than in the SHAM group. In the hindbrain, the following regions showed a significant positive difference in the FDG signal: several tegmental areas including ventral tegmental, pedunculopontine and dorsomedial areas (Fig. 2F, H, and I), dorsal raphe (DR; Fig. 2I), parabrachial nucleus (PB; Fig. 2J) and the locus coeruleus (LC; Fig. 2K). These brain regions are considered to contain abundant neurons that release catecholamines and monoamines such as noradrenaline, dopamine, and serotonin. In addition to these regions, the following nuclei showed a larger increase in FDG uptake in the CTA group than in the SHAM group: the medial septal nucleus, septohypothalamic nucleus (Fig. 2A), gigantocellular reticular nucleus (Fig. 2C), pararubral nucleus (Fig. 2G) and ventrolateral periaqueductal gray matter (vlPAG; Fig. 2J).

3. Subtraction of Day1 saccharin intake from Day3 saccharin intake of the CTA group

Another subtraction analysis was performed to demonstrate the CTA-related brain region, i.e., PET images from Day1 of the CTA group were subtracted from those from Day3 of the same treatment group (Fig. 3). Although the subtraction of Day3-Day1 in CTA possibly regions related to accommodation to saccharin intake, this also involves CTA-related regions as well as CTA-SHAM on Day3.

In these images, the hippocampus, PaS, and pre- and postsubiculum showed significantly larger increases in the uptake of FDG among the limbic system (Fig. 3A and B). In the cerebral cortex, the entorhinal cortex (Ent) also showed larger increases in FDG uptake (Fig. 3B). In the hindbrain, DR and PB showed larger increases in FDG uptake (Fig. 3B and C).

4. Subtraction of the NaCl group from the LiCl group

The detected regions in the subtraction of Day3 of the SHAM group from the Day3 of the CTA group described above might be related to the LiCl-induced responses such as nociception, nausea, and malaise that the CTA group experienced on Day2 by the LiCl i.p. injection in combination with the IOAS. To identify the LiCl-related regions, we performed PET imaging just after the LiCl or saline i.p. injection and subtracted FDG uptake after the saline i.p. injection from that after the LiCl i.p. injection.

The larger uptake of FDG responding to the LiCl injection (the LiCl group) in comparison to that of the saline injection (the NaCl group) was detected in the ventral part of the primary somatosensory and secondary somatosensory cortices (Fig. 4B and C). These regions are likely to involve the lip and jaw regions (Nakamura, Kato, Shirakawa, Koshikawa, & Kobayashi, 2015; Remple, Henry, & Catania, 2003) and visceral area of the IC (Yasui et al., 1991). In addition to these somatosensory cortices, the agranular and dysgranular IC also exhibited a larger FDG uptake in the LiCl group than the NaCl group (Fig. 4A). In addition to the cerebral cortex, the PB showed a larger FDG uptake in the LiCl group than the NaCl group (Fig. 4D).

These results suggest that the brain regions that showed the larger uptake of FDG responding to the LiCl injection correspond to related regions.

5. Subtraction of Day1 of the IOAS group from Day3 of the IOAS group

The detected regions in the subtraction of Day1 of the IOAS group from Day3 of the IOAS group described above might be related to the saccharin-induced responses such as habituation, memory, and reward that the IOAS group experienced on Day2.

The larger uptake of FDG responding to the IOAS on Day3 in comparison to that of Day1 was detected in globus pallidus (GP; Fig. 5B). This region is likely to involve in the reward system including dopaminergic input from the substantia nigra through the striatum. Furthermore, the parasubiculum (PaS; Fig5C) also exhibited a larger FDG uptake in Day3 than Day1. This region participates in memory and learning. In addition to these regions, the following nuclei showed a larger increase in FDG uptake in Day3 than Day1: the primary somatosensory (SI; Fig. 5A), and dorsal part of the inferior colliculus (DPIC; Fig. 5C), which has been reported to receive auditory information and integrate multiple sensations. These regions are likely to involve in the sensory of IOAS.

These results suggest that these regions participate in memory for saccharin.

Discussion

In comparison to histological studies focusing on c-Fos and phosphorylated ERK, the present PET study using a subtraction method has the advantage of more direct evaluation of changes in neural activities by CTA using the same animals. This direct evaluation of CTA-related activativation in the nuclei of neuromodulators strengthen the evidence that neuromodulators including serotonergic, adrenergic, dopaminergic, and cholinergic systems cooperatively contribute to the induction of CTA.

In the present study, we analyzed FDG-PET images obtained from the following subtraction: 1) Day 3 images of the SHAM group subtracted from those of the CTA group (Fig. 2), 2) Day1 images subtracted from Day3 images of the CTA group, and 3) images of the NaCl group subtracted from the LiCl group. By using the subtraction method, we demonstrated the activation of nuclei that produce neuromodulators (acetylcholine, noradrenaline, serotonin, and dopamine), in addition to the hippocampus and several other related brain regions, in response to CTA retrieval.

1. The strategy for detecting brain regions from CTA-related imaging

By using the previously discussed advantages of FDG-PET, the imaging method for visualizing brain-wide activities under the free-moving condition, we could image Day3 of the CTA group with the observation of specific disgust behaviors, indicating that we positively imaged the rats with CTA. In the free moving rat, the IOAS induces neural activities that code not only gustation but also somatosensation and motor activities. Such

complex information induces neural activation in various brain regions, which may overlap and, as a result, mask the brain regions that process specific information, such as imaging in this case. The present study used the subtraction method, which enables us to identify the brain activities relating to the CTA imaging process by canceling gustatory information processing induced by the IOAS. As a result, the subtraction images of CTA-SHAM groups on Day3 likely reveal the image processing of negative feelings that the CTA group experienced a day before the second PET scanning, and the subtraction images of LiCl-NaCl groups reveal the actual sensation such as pain and malaise caused by i.p. injection of LiCl.

2. Activation of the pain-related regions without pain in the CTA group

In the subtraction of CTA-SHAM groups on Day3, several pain-related brain regions including Sol, PB, and IC, which are considered to process multimodal sensation such as gustation and nociception (Cechetto, 2014), were activated even though no nociceptive stimulus was applied in the CTA groups. The Sol receives somatosensory and gustatory information from the primary afferents including the glossopharyngeal and vagal nerves (Yamamoto, 1984), and Sol neurons project to the PB and/or higher brain regions such as the thalamic nuclei and amygdala (Jia, Rao, & Shi, 1994). A part of the IC, the granular and dysgranular IC caudally adjacent to the middle cerebral artery, responds to mechanical stimulation of the internal organs (Hanamori, Kunitake, Kato, & Kannan, 1998; Kobayashi, 2011). Previous immunohistochemical studies demonstrated that the i.p. administration of LiCl induces c-Fos protein in the IC, PB, and Sol (Swank, & Bernstein 1994; Soto, Gasalla,

Begega, & López, 2017), which suggests that these brain regions are activated by the i.p. injection of LiCl.

Therefore, a possible explanation for this finding is that the imaging displays the negative feeling including pain experienced by the rats induced by the i.p. injection of LiCl as the US in combination with the CS, i.e. IOAS, a day before PET scanning. If this is the case, the i.p. injection of LiCl is likely to activate pain-related regions including the IC, PB, and Sol. Indeed, the subtraction PET images of the saline injection from the i.p. injection of LiCl showed the activation of agranular and dysgranular IC, PB, primary and secondary somatosensory cortices (Fig. 4), which corresponded to disgust behaviors such as freezing, rearing, and gaping after the LiCl injection. However, there is a discrepancy in that the Sol was not detected in the subtraction images of the saline injection from the LiCl injection, though the Sol also relates to visceral pain (Gamboa-Esteves, Lima, & Batten, 2001). Furthermore, the uptake of FDG in the PB was observed in the subtraction imaging of Day1 from Day3 of the CTA group. We considered that the responding areas may disappear due to the subtraction method. The subtraction method allows us to examine only the activated brain regions during saccharin solution-intake from the rats that established CTA. Therefore, if the Sol responds to saccharin intake, the difference of the Sol activities between saline and LiCl injection might be masked. Indeed, the Sol neurons receive not only nociceptive information but also gustatory information from the taste fibers (Yamamoto, 1984).

In the nociceptive information processing, the ascending information from the peripheral nerves to the central nervous system and the descending inputs to the pain-related brain regions have been reported (Ren & Dubner, 2002). One of the principal targets of these

descending inputs is the vlPAG, from which excitatory glutamatergic axons project to the DR and LC (Behbehani, 1995). These pathways are hypothesized to suppress pain, and the present results of activation both in the vlPAG and DR/LC may reflect the activation of the descending pathways during CTA retrieval.

3. Memory retrieval

In addition to activation of the visceral sensation-related brain regions described above, the subtraction images of Day1 from Day3 in the CTA group reveal the significant increases in PaS, pre- and postsubiculum in the hippocampus and Ent (Fig. 3). Osorio-Gomez et al. (2023) reviewed the brain regions that contribute to the retrieval process including consciously retrieving details of the context in which the stimulus occurred: the hippocampus, Ent, prefrontal, perirhinal, insular, and postrhinal cortices. The present results of activation in the hippocampus and Ent partially replicate their study. Ent is reciprocally connected to the hippocampus (Deadwyler, West, Cotman, & Lynch, 1975) and is considered to be involved in temporal association memory as well as the hippocampus (Suh, Rivest, Nakashiba, Tominaga, & Tonegawa, 2011). The hypothesis that the retrieval process of CTA is detected in the subtraction images of Day1 from Day3 in the CTA group may be supported by this activation pattern, i.e., memory-related regions: the CS, saccharin solution-intake, may induce the top-down signal from the prefrontal cortex and recall the memory of visceral sensation, which results in the activation of the pain-related region in the brain without real LiCl stimulation. The present finding of the activation of the ventral hippocampus and adjacent Ent is in the line with the report that chemical lesions of the whole but not dorsal

hippocampus impair CTA retention (Yamamoto, Fujimoto, Shimura, & Sakai, 1995). On the other hand, we found insignificant activation in the amygdala, which is known to be activated during CTA retrieval (Miranda et al., 2003b). The amygdala receives not only taste information but also visual, auditory, somatosensory, and olfactory information via the thalamus and cerebral cortex. Therefore, there is a possibility that activities in the amygdala on Day1 of the CTA group are relatively high, which may cancel a significant increase in the subtraction of Day1 from Day3.

4. Neuromodulatory systems activated by CTA

The present results obtained from the CTA-SHAM groups suggest that the retrieval process accompanies the activation of neuromodulatory systems: serotonergic, dopaminergic, cholinergic, and adrenergic systems. There are at least two possibilities for the activation mechanisms of neuromodulatory systems, the CTA retrieval process itself or pain control, which have been reported to accompany the activation of several neuromodulatory systems as described below.

4.1. Dorsal raphe and locus coeruleus

The LC and raphe nucleus are also targets in the study of CTA and were active in our study during taste aversion. These regions are part of the brain stem and have dense neurons releasing noradrenaline and serotonin, respectively.

Serotonin has been reported to be involved in LiCl-induced CTA in various aspects such as acquisition and retention. Systemic application of 5-HT_{1A} antagonists attenuates

LiCl-induced CTA (Wegener, Smith, & Rosenberg, 1997), and a 5-HT_3 antagonist injection in the anterior but not in the posterior IC reduces the establishment of LiCl-induced CTA (Tuerke, Limebeer, Fletcher, & Parker, 2012). It is also noted that saccharin application to rats that have developed CTA increases serotonin in the hypothalamus but not in the hippocampus (West, Mark, & Hoebel, 1991). Although there are contradictory studies reporting that CTA is enhanced by electrolytic lesions of the DR and median raphe nuclei (Lorden & Margules, 1977), while chemical lesions of these nuclei by 5,7-dihydroxytryptamine has little effect on CTA (Limebeer, Parker, & Fletcher, 2004), these previous reports support the present finding of DR activation in the subtraction of the SHAM group from the CTA group.

The roles of noradrenaline in CTA have been mainly focused on the amygdala. Blockade of β-adrenergic receptors in the basolateral amygdala just before the LiCl i.p. injection or just after pre-exposure to saccharin as the CS disrupts CTA memory (Miranda, Ferreira, Ramirez-Lugo, & Bermudez-Rattoni, 2003). In addition, noradrenaline release is increased by novel saccharin intake 45 min after CTA acquisition (Guzman-Ramos, Osorio-Gomez, Moreno-Castilla, & Bermudez-Rattoni, 2012). An α_2-adrenoceptor antagonist i.p. injection suppresses CTA retention (Ishitobi et al., 2009). Recently, a study demonstrated that selective stimulation of the LC noradrenergic neurons by a chemogenetic approach enhances the retrieval of CTA via α_1- and β-adrenoceptors in the basolateral amygdala (Fukabori et al., 2020). These previous reports support the present finding of LC activation in the subtraction of the SHAM group from the CTA group.

4.2. Substantia nigra and ventral tegmental area

Previous studies of deletion of dopaminergic fibers by 6-OHDA (Berridge & Robinson, 1998), knockout of dopaminergic receptors (Cannon, Scannell, & Palmiter, 2005), or pharmacological manipulation of dopaminergic receptors by the systemic administration of dopaminergic ligands (Asin & Montana, 1989; Fenu, Bassareo, & Di Chiara, 2001; Mediavilla, Mahia, Bernal, & Puerto, 2012) have demonstrated the involvement of the dopaminergic system in CTA. In addition to these systemic roles of dopamine in CTA, several specific brain regions, such as the NAc (Fenu, Bassareo, & Di Chiara, 2001; Miranda et al., 2017), the gustatory area of the IC (Guzman-Ramos & Bermudez-Rattoni, 2011), the medial prefrontal cortex (Gonzalez et al., 2014), the amygdala (Guzman-Ramos, Osorio-Gomez, Moreno-Castilla, & Bermudez-Rattoni, 2010), and the PB (Zach, Krivanek, & Vales, 2006), have been focused on to examine roles of the dopaminergic system in CTA. With a focus on the dopaminergic contribution in the post-CTA period, dopamine release responding to saccharin application to the NAc of the rats with CTA is less than that of the rats without CTA (Mark, Blander, & Hoebel, 1991). On the other hand, dopamine in the IC of the rats with CTA increases in response to saccharin, which is blocked by a 6-cyano-7-nitroquinoxaline-2,3-dione application in the amygdala (Osorio-Gomez, Guzman-Ramos, & Bermudez-Rattoni, 2017). These microdialysis studies suggest different regulation mechanisms of dopamine release responding to saccharin after CTA acquisition according to brain regions. These results suggest an involvement of the dopaminergic system in CTA processing, though Berridge and Robinson (1998) demonstrated comparable rates of the aversive and hedonic reaction to saccharin application between the rats with and without

deletion of dopaminergic fibers. The subtraction of the SHAM group from the CTA group in the present study demonstrated activation of both the substantia nigra and ventral tegmental area, whose principal roles in physiological function are motor and aversion-related behaviors, respectively (Smith & Masilamoni, 2010; Morales & Margolis, 2017). Therefore, these subtraction images may represent dopaminergic activation in response to the increased orofacial movements such as gnawing and tongue-protrusion and the emotional activities responding to recall of visceral sensation induced by LiCl injection, respectively.

4.3. Basal forebrain

We observed more uptake of FDG in the NBM and septal nucleus, which compose the basal forebrain. Bermúdez-Rattoni and his colleagues reported on the cholinergic roles in CTA, especially focusing on the IC (Miranda, Ferreira, Ramirez-Lugo, & Bermudez-Rattoni, 2003). The CTA acquisition process needs neural activities of the NBM, which increases acetylcholine release in the IC, whereas the amount of acetylcholine in the IC is not changed during the retrieval process that is carried out 10 days after CTA acquisition (Miranda & Bermudez-Rattoni, 1999). Similarly, the injection of an M_1/M_3 receptor antagonist into the IC during the acquisition process inhibits CTA, and that during the retrieval process does not change CTA (Ramirez-Lugo, Miranda, Escobar, Espinosa, & Bermudez-Rattoni, 2003). These results suggest that the cholinergic system is activated during the CTA acquisition process but not during the retrieval process. On the other hand, the release amount of acetylcholine in the NAc increases in response to the saccharin application in the rats with CTA (Mark, Weinberg, Rada, & Hoebel, 1995). Therefore, not only the CTA acquisition

process but also the retrieval process activates the cholinergic system in the brain. This matches our present results.

5. Conclusions

Responding to the IOAS, the whole brain imaging using FDG-PET demonstrated increased neural activities of the neuromodulatory systems including serotonin, noradrenaline, dopamine, and acetylcholine in rats with CTA compared to rats without CTA. In addition, pain-related brain regions such as the PB and the PAG showed increased activation in the rats with CTA despite no nociceptive stimulation. These findings suggest a coordinated activation of the neuromodulatory systems during CTA retrieval.

Acknowledgements

I am grateful to Prof. Masayuki Kobayashi for the opportunity to perform this study and his instructions for this study. I would like to thank the colleagues in Department of Pharmacology and RIKEN Center for Molecular Imaging Science for their technical advice and assistance.

References

Asin, K.E., Montana, W.E., 1989. Studies on D1 and D2 dopamine receptor involvement in conditioned taste aversions. Pharmacol Biochem Behav. 32, 1033-1041. 10.1016/0091-3057(89)90077-4

Behbehani, M.M., 1995. Functional characteristics of the midbrain periaqueductal gray. Prog Neurobiol. 46, 575-605. 10.1016/0301-0082(95)00009-k

Berridge, K.C., Robinson, T.E., 1998. What is the role of dopamine in reward: hedonic impact, reward learning, or incentive salience? Brain Res Brain Res Rev. 28, 309-369. 10.1016/s0165-0173(98)00019-8

Cannon, C.M., Scannell, C.A., Palmiter, R.D., 2005. Mice lacking dopamine D1 receptors express normal lithium chloride-induced conditioned taste aversion for salt but not sucrose. Eur J Neurosci. 21, 2600-2604. 10.1111/j.1460-9568.2005.04077.x

Cechetto, D.F., 2014. Cortical control of the autonomic nervous system. Exp Physiol. 99, 326-331. 10.1113/expphysiol.2013.075192

Deadwyler, S.A., West, J.R., Cotman, C.W., Lynch, G., 1975. Physiological studies of the reciprocal connections between the hippocampus and entorhinal cortex. Exp Neurol. 49, 35-57. 10.1016/0014-4886(75)90194-6

Dunn, L.T., Everitt, B.J., 1987. The effects of lesions to noradrenergic projections from the locus coeruleus and lateral tegmental cell groups on conditioned taste aversion in the rat. Behav Neurosci. 101, 409-422. 10.1037//0735-7044.101.3.409

Fenu, S., Bassareo, V., Di Chiara, G., 2001. A role for dopamine D1 receptors of the nucleus accumbens shell in conditioned taste aversion learning. J Neurosci. 21, 6897-6904. 10.1523/JNEUROSCI.21-17-06897.2001

Fukabori, R., et al., 2020. Enhanced Retrieval of Taste Associative Memory by Chemogenetic Activation of Locus Coeruleus Norepinephrine Neurons. J Neurosci. 40, 8367-8385. 10.1523/JNEUROSCI.1720-20.2020

Gamboa-Esteves, F.O., Lima, D., Batten, T.F., 2001. Neurochemistry of superficial spinal neurones projecting to nucleus of the solitary tract that express c-fos on chemical somatic and visceral nociceptive input in the rat. Metab Brain Dis. 16, 151-164. 10.1023/a:1012536910214

Gonzalez, M.C., Kramar, C.P., Tomaiuolo, M., Katche, C., Weisstaub, N., Cammarota, M., Medina, J.H., 2014. Medial prefrontal cortex dopamine controls the persistent storage of aversive memories. Front Behav Neurosci. 8, 408. 10.3389/fnbeh.2014.00408

Grill, H.J., Norgren, R., 1978. The taste reactivity test. I. Mimetic responses to gustatory stimuli in neurologically normal rats. Brain Res. 143, 263-279. 10.1016/0006-8993(78)90568-1

Guzman-Ramos, K., Osorio-Gomez, D., Moreno-Castilla, P., Bermudez-Rattoni, F., 2010. Off-line concomitant release of dopamine and glutamate involvement in taste memory consolidation. J Neurochem. 114, 226-236. 10.1111/j.1471-4159.2010.06758.x

Guzman-Ramos, K., Bermudez-Rattoni, F., 2011. Post-learning molecular reactivation underlies taste memory consolidation. Front Syst Neurosci. 5, 79. 10.3389/fnsys.2011.00079

Guzman-Ramos, K., Osorio-Gomez, D., Moreno-Castilla, P., Bermudez-Rattoni, F., 2012. Post-acquisition release of glutamate and norepinephrine in the amygdala is involved in taste-aversion memory consolidation. Learn Mem. 19, 231-238. 10.1101/lm.024703.111

Hanamori, T., Kunitake, T., Kato, K., Kannan, H., 1998. Responses of neurons in the insular cortex to gustatory, visceral, and nociceptive stimuli in rats. J Neurophysiol. 79, 2535-2545. 10.1152/jn.1998.79.5.2535

Inui, T., Yamamoto, T., Shimura, T., 2009. GABAergic transmission in the rat ventral pallidum mediates a saccharin palatability shift in conditioned taste aversion. Eur J Neurosci. 30, 110-115. 10.1111/j.1460-9568.2009.06800.x

Ishitobi, S., Ayuse, T., Yoshida, H., Oi, K., Toda, K., Miyamoto, T., 2009. Effects of midazolam on acquisition and extinction of conditioned taste aversion memory in rats. Neurosci Lett. 450, 270-274. 10.1016/j.neulet.2008.11.044

Jia, H.G., Rao, Z.R., Shi, J.W., 1994. An indirect projection from the nucleus of the solitary tract to the central nucleus of the amygdala via the parabrachial nucleus in the rat: a light and electron microscopic study. Brain Res. 663, 181-190. 10.1016/0006-8993(94)91262-9
Kobayashi, M., 2011. Macroscopic connection of rat insular cortex: anatomical bases underlying its physiological functions. Int Rev Neurobiol. 97, 285-303. 10.1016/B978-0-12-385198-7.00011-4

Kobayashi, M., Cui, Y., Sako, T., Sasabe, T., Mizoguchi, N., Yamamoto, K., Wada, Y., Kataoka, Y., Koshikawa, N., 2013. Functional neuroimaging of aversive taste-related areas in the alert rat revealed by positron emission tomography. J Neurosci Res. 91, 1363-1370. 10.1002/jnr.23252

Likhtik, E., Johansen, J.P., 2019. Neuromodulation in circuits of aversive emotional learning. Nat Neurosci. 22, 1586-1597. 10.1038/s41593-019-0503-3

Limebeer, C.L., Parker, L.A., Fletcher, P.J., 2004. 5,7-dihydroxytryptamine lesions of the dorsal and median raphe nuclei interfere with lithium-induced conditioned gaping, but not conditioned taste avoidance, in rats. Behav Neurosci. 118, 1391-1399. 10.1037/0735-7044.118.6.1391

Lopez-Garcia, J.C., Fernandez-Ruiz, J., Escobar, M.L., Bermudez-Rattoni, F., Tapia, R., 1993. Effects of excitotoxic lesions of the nucleus basalis magnocellularis on conditioned taste aversion and inhibitory avoidance in the rat. Pharmacol Biochem Behav. 45, 147-152. 10.1016/0091-3057(93)90098-e

Lorden, J.F., & Margules, D.L., 1977. Enhancement of conditioned taste aversions by lesions of the midbrain raphe nuclei that deplete serotonin. Physiol Psychol. 5, 273-279. 10.3758/BF03335330

Mark, G.P., Blander, D.S., Hoebel, B.G., 1991. A conditioned stimulus decreases extracellular dopamine in the nucleus accumbens after the development of a learned taste aversion. Brain Res. 551, 308-310. 10.1016/0006-8993(91)90946-s

Mark, G.P., Weinberg, J.B., Rada, P.V., Hoebel, B.G., 1995. Extracellular acetylcholine is increased in the nucleus accumbens following the presentation of an aversively conditioned taste stimulus. Brain Res. 688, 184-188. 10.1016/0006-8993(95)00401-b

Meachum, C.L., Bernstein, I.L., 1992. Behavioral conditioned responses to contextual and odor stimuli paired with LiCl administration. Physiol Behav. 52, 895-899. 10.1016/0031-9384(92)90368-c

Mediavilla, C., Mahia, J., Bernal, A., Puerto, A., 2012. The D2/D3-receptor antagonist tiapride impairs concurrent but not sequential taste aversion learning. Brain Res Bull. 87, 346-349. 10.1016/j.brainresbull.2011.10.022

Miranda, M.I., Bermudez-Rattoni, F., 1999. Reversible inactivation of the nucleus basalis magnocellularis induces disruption of cortical acetylcholine release and acquisition, but not retrieval, of aversive memories. Proc Natl Acad Sci USA. 96, 6478-6482. 10.1073/pnas.96.11.6478

Miranda, M.I., Ferreira, G., Ramirez-Lugo, L., Bermudez-Rattoni, F., 2003a. Role of cholinergic system on the construction of memories: taste memory encoding. Neurobiol Learn Mem. 80, 211-222. 10.1016/s1074-7427(03)00061-3

Miranda, M.I., LaLumiere, R.T., Buen, T.V., Bermudez-Rattoni, F., McGaugh, J.L., 2003b. Blockade of noradrenergic receptors in the basolateral amygdala impairs taste memory. Eur J Neurosci. 18, 2605-2610. 10.1046/j.1460-9568.2003.03008.x

Miranda, M.I., Rangel-Hernandez, J.A., Vera-Rivera, G., Garcia-Medina, N.E., Soto-Alonso, G., Rodriguez-Garcia, G., Nunez-Jaramillo, L., 2017. The role of dopamine D2 receptors in the nucleus accumbens during taste-aversive learning and memory extinction after long-term sugar consumption. Neuroscience. 359, 142-150. 10.1016/j.neuroscience.2017.07.009

Morales, M., Margolis, E.B., 2017. Ventral tegmental area: cellular heterogeneity, connectivity and behaviour. Nat Rev Neurosci. 18, 73-85. 10.1038/nrn.2016.165

Nakamura, H., Kato, R., Shirakawa, T., Koshikawa, N., Kobayashi, M., 2015. Spatiotemporal profiles of dental pulp nociception in rat cerebral cortex: An optical imaging study. J Comp Neurol. 523, 1162-1174. 10.1002/cne.23692

Osorio-Gomez, D., Guzman-Ramos, K., Bermudez-Rattoni, F., 2017. Memory trace reactivation and behavioral response during retrieval are differentially modulated by amygdalar glutamate receptors activity: interaction between amygdala and insular cortex. Learn Mem. 24, 14-23. 10.1101/lm.042895.116

Osorio-Gomez, D., Miranda, M.I., Guzman-Ramos, K., Bermudez-Rattoni, F., 2023. Transforming experiences: Neurobiology of memory updating/editing. Front Syst Neurosci. 17, 1-14. 10.3389/fnsys.2023.1103770

Paxinos, G., Watson, C., 2007. The Rat Brain in Stereotaxic Coordinates, 6th ed. San Diego: Academic Press.

Ramirez-Lugo, L., Miranda, M.I., Escobar, M.L., Espinosa, E., Bermudez-Rattoni, F., 2003. The role of cortical cholinergic pre- and post-synaptic receptors in taste memory formation. Neurobiol Learn Mem. 79, 184-193. 10.1016/s1074-7427(02)00038-2

Remple, M.S., Henry, E.C., Catania, K.C., 2003. Organization of somatosensory cortex in the laboratory rat (Rattus norvegicus): Evidence for two lateral areas joined at the representation of the teeth. J Comp Neurol. 467, 105-118. 10.1002/cne.10909

Ren, K., Dubner, R., 2002. Descending modulation in persistent pain: an update. Pain. 100, 1-6. 10.1016/s0304-3959(02)00368-8

Schiffer, W.K., Mirrione, M.M., Dewey, S.L., 2007. Optimizing experimental protocols for quantitative behavioral imaging with 18F-FDG in rodents. J Nucl Med. 48, 277-287.

Schweinhardt, P., Fransson, P., Olson, L., Spenger, C., Andersson, J.L., 2003. A template for spatial normalisation of MR images of the rat brain. J Neurosci. 129, 105-113. 10.1016/s0165-0270(03)00192-4

Smith, Y., Masilamoni, J.G., 2010. Substantia Nigra. In Kompoliti, K., & Verhagen, L. (Eds.), Encyclopedia of Movement Disorders, 1st ed. San Diego: Academic Press, pp. 189-192

Soto, A., Gasalla, P., Begega, A., López, M., 2017. c-Fos activity in the insular cortex, nucleus accumbens and basolateral amygdala following the intraperitoneal injection of saccharin and lithium chloride. Neurosci Lett. 647, 32-37. 10.1016/j.neulet.2017.03.025

Suh, J., Rivest, A.J., Nakashiba, T., Tominaga, T., Tonegawa, S., 2011. Entorhinal cortex layer III input to the hippocampus is crucial for temporal association memory. Science. 334, 1415-1420. 10.1126/science.1210125

Swank, M.W., Bernstein, I.L.,1994. c-Fos induction in response to a conditioned stimulus after single trial taste aversion learning. Brain Res. 636, 202-208. 10.1016/0006-8993(94)91018-9

Tuerke, K.J., Limebeer, C.L., Fletcher, P.J., Parker, L.A., 2012. Double dissociation between regulation of conditioned disgust and taste avoidance by serotonin availability at the 5-HT(3) receptor in the posterior and anterior insular cortex. J Neurosci. 32, 13709-13717. 10.1523/JNEUROSCI.2042-12.2012

Wegener, G., Smith, D.F., Rosenberg, R., 1997. 5-HT_{1A} receptors in lithium-induced conditioned taste aversion. Psychopharmacology (Berl). 133, 51-54. 10.1007/s002130050370

West, H.L., Mark, G.P., Hoebel, B.G., 1991. Effects of conditioned taste aversion on extracellular serotonin in the lateral hypothalamus and hippocampus of freely moving rats. Brain Res. 556, 95-100. 10.1016/0006-8993(91)90551-6

Yamamoto, T., 1984. Taste responses of cortical neurons. Prog Neurobiol. 23, 273-315. 10.1016/0301-0082(84)90007-8

Yamamoto, T., Fujimoto, Y., Shimura, T., Sakai, N., 1995. Conditioned taste aversion in rats with excitotoxic brain lesions. Neurosci Res. 22, 31-49. 10.1016/0168-0102(95)00875-t

Yamamoto, T., Nagai, T., Shimura, T., Yasoshima, Y., 1998. Roles of chemical mediators in the taste system. Jpn J Pharmacol. 76, 325-348. 10.1254/jjp.76.325

Yasui, Y., Breder, C.D., Saper, C.B., Cechetto, D.F., 1991. Autonomic responses and efferent pathways from the insular cortex in the rat. J Comp Neurol. 303, 355-374. 10.1002/cne.903030303

Zach, P., Krivanek, J., Vales, K., 2006. Serotonin and dopamine in the parabrachial nucleus of rats during conditioned taste aversion learning. Behav Brain Res. 170, 271-276. 10.1016/j.bbr.2006.03.001

Figures

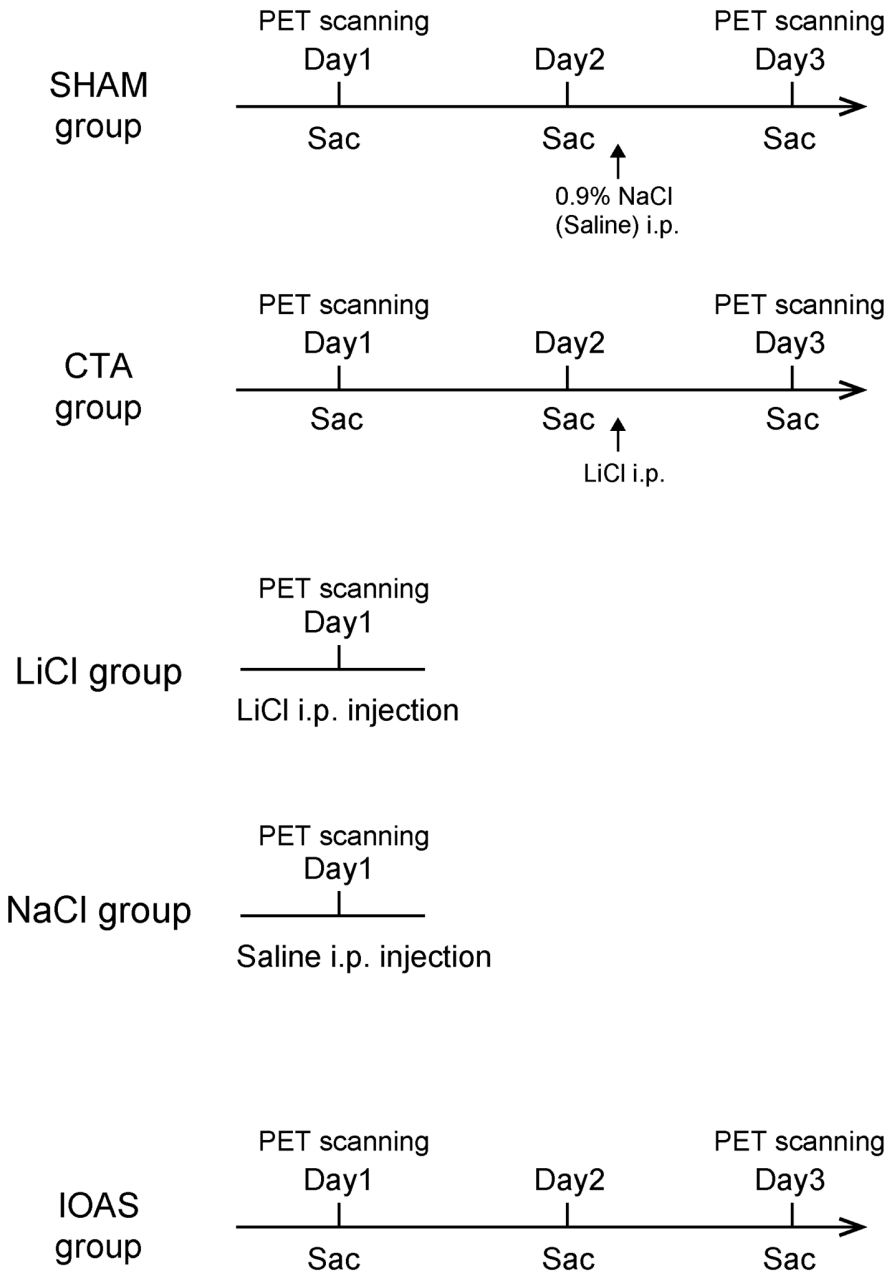

Figure 1. Experimental paradigms. The rats that received PET imaging were divided into 5 groups. The SHAM and CTA groups were scanned just after IOAS on Day1 and Day3. On Day2, the SHAM and CTA groups received the i.p. injection of 0.9% NaCl and LiCl, respectively, with the IOAS. The LiCl and NaCl groups were scanned after the i.p. injection of LiCl and NaCl, respectively. The IOAS groups were scanned just after IOAS on Day1 and Day3.

CTA – SHAM on Day3

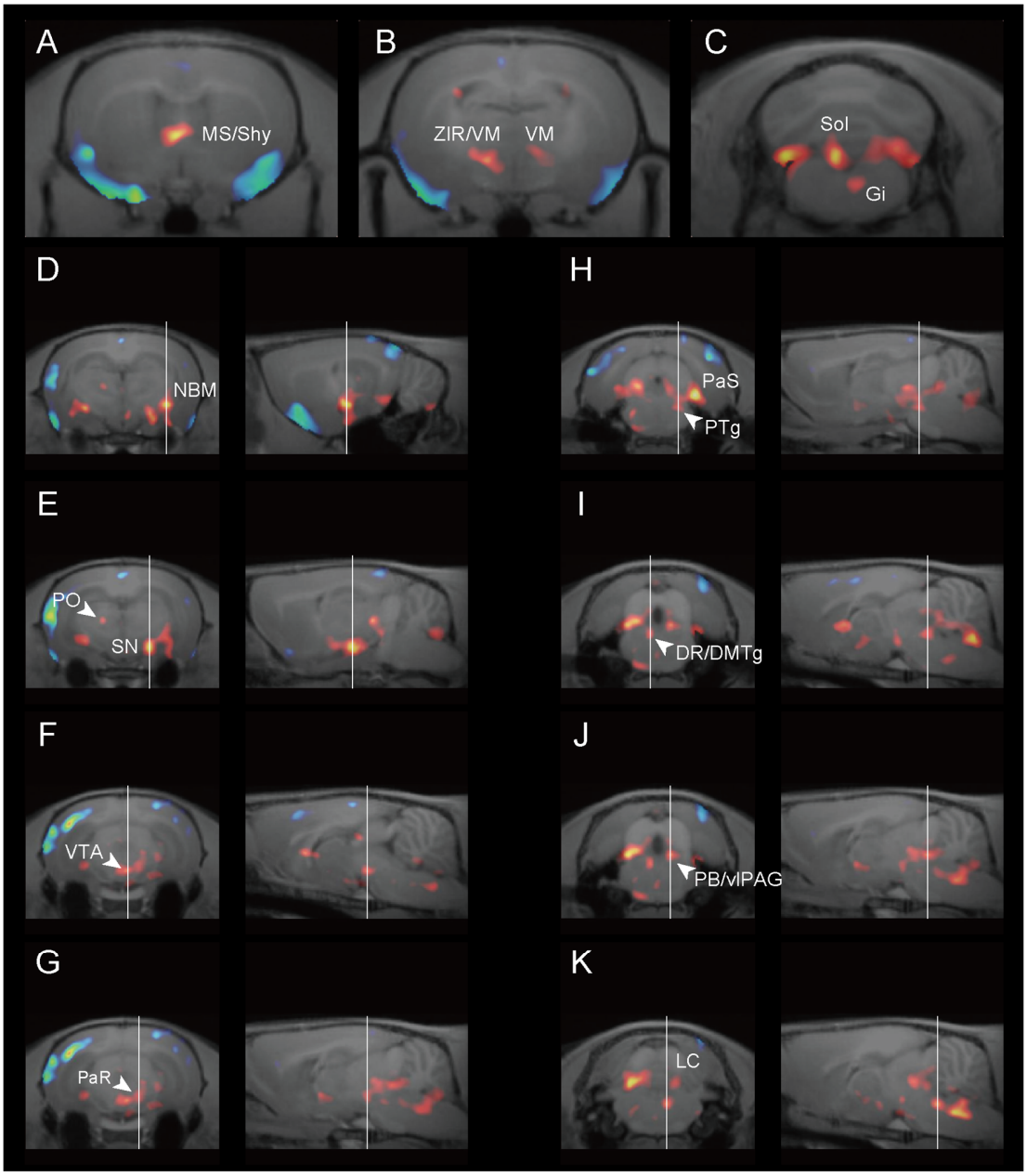

Figure 2. Areas of activation in response to saccharin intake of CTA conditioned rats superimposed upon coronal and sagittal slices. Images were obtained by the subtraction of Day3 of the SHAM group from Day3 of the CTA group. The range of *T*-values coded in the color scale was applied for all images. DMTg, dorsomedial tegmental area; DR, dorsal raphe; Gi, gigantocellular reticular nucleus; LC, locus coeruleus; MS, medial septal nucleus; PaR, pararubral nucleus; PaS, parasubiculum; PB, parabrachial nucleus; PO, posterior thalamic nuclear group; PTg, pedunculopontine tegmental nucleus; Shy, septohypothalamic nucleus; SN, substantia nigra; Sol, solitary nucleus; vlPAG, ventrolateral periaqueductal gray matter; VM, ventromedial thalamic nucleus; VTA, ventral tegmental area; ZIR, zona incerta. The vertical white lines indicate the location of coronal and sagittal slices. The *T*-value of 3.45 used as the threshold in the figure corresponds to the $P < 0.001$ (uncorrected) threshold described in the text. Right in the presented images corresponds to the right hemisphere.

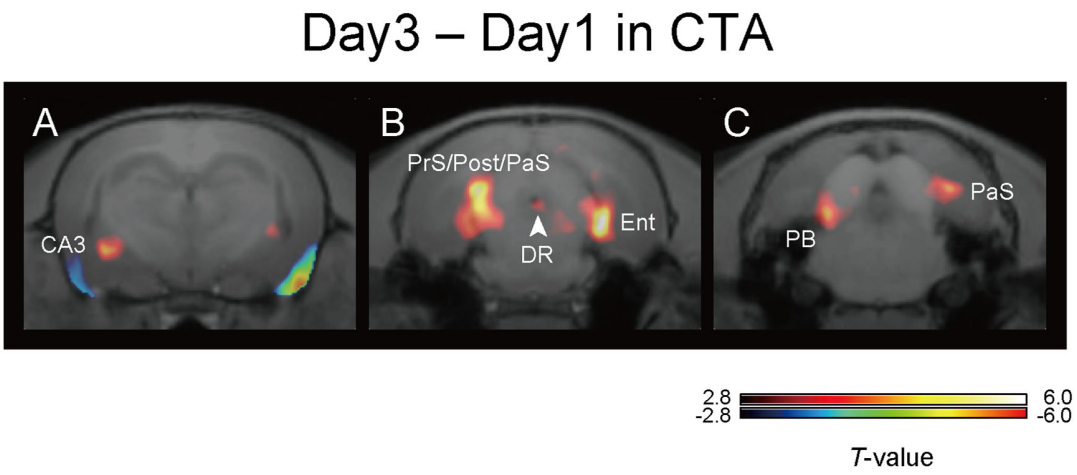

Figure 3. Areas of activation in response to saccharin intake of CTA conditioned rats superimposed upon coronal slices. Images were obtained by the subtraction of Day1 of the CTA group from Day3 of the same group. The range of *T*-values coded in the color scale was applied for all images. Ent, entorhinal cortex; OB, olfactory bulb; Post, postsubiculum; PrS, presubiculum. The *T*-value of 3.55 used as the threshold in the figure corresponds to the $P < 0.001$ (uncorrected) threshold described in the text. Right in the presented images corresponds to the right hemisphere.

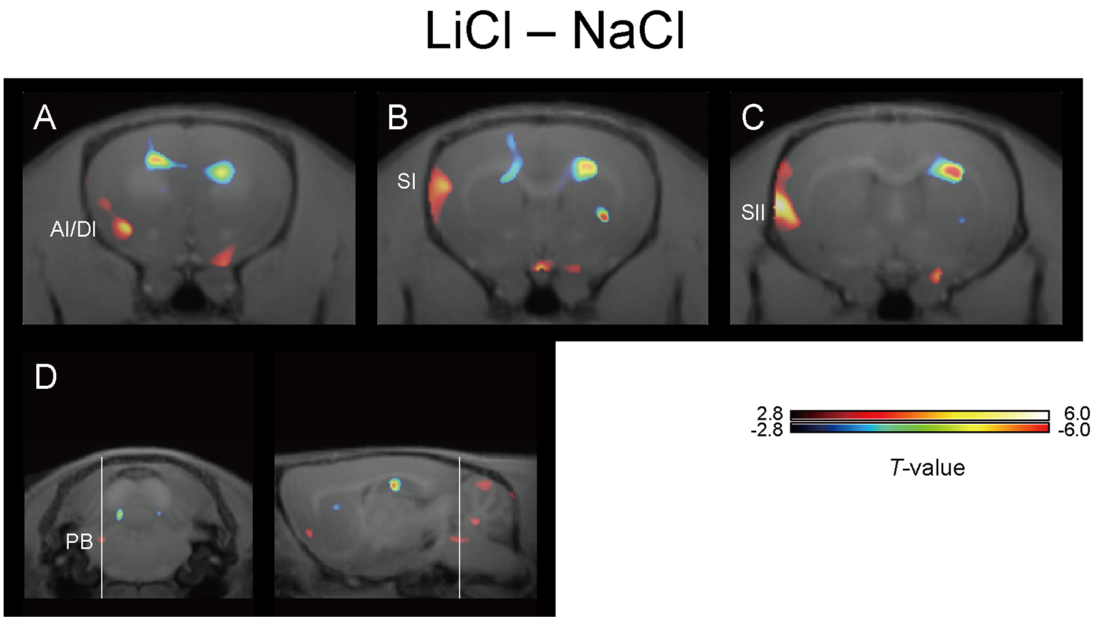

Figure 4. Areas of larger activation in response to the i.p. injection of LiCl than the saline injection superimposed upon coronal and sagittal slices. Images were obtained by the subtraction of the saline injection from the LiCl injection. The range of *T*-values coded in the color scale was applied for all images. AI, agranular cortex; DI, dysgranular cortex; SI, primary somatosensory cortex; SII, secondary somatosensory cortex. The *T*-value of 2.92 used as the threshold in the figure corresponds to the $P < 0.005$ (uncorrected) threshold described in the text. Right in the presented images corresponds to the right hemisphere.

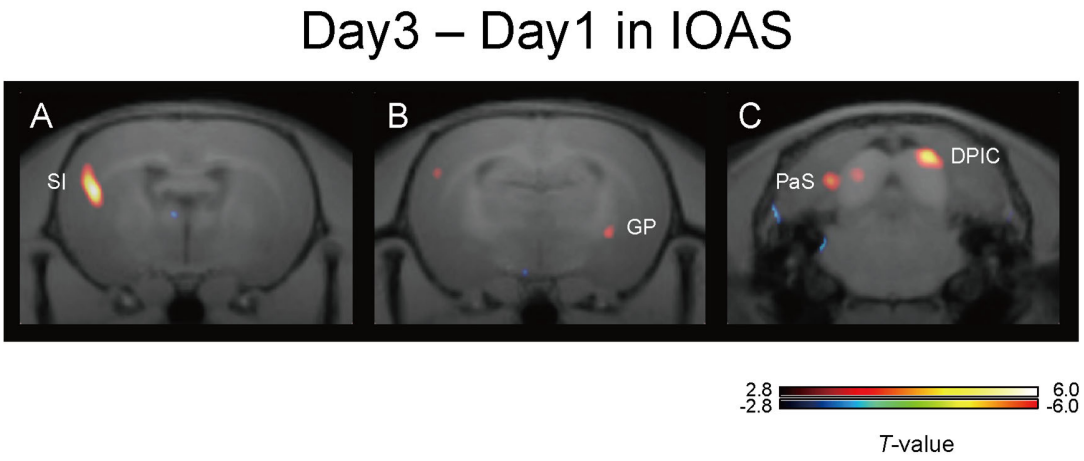

Figure 5. Areas of activation in response to saccharin intake of naive rats superimposed upon coronal slices. Images were obtained by the subtraction of Day1 of the IOAS group from Day3 of the IOAS group. The range of *T*-values coded in the color scale was applied for all images. SI, primary somatosensory cortex; GP, globus pallidus; PaS, parasubiculum; DPIC, dorsal part of the inferior colliculus. The *T*-value of 2.92 used as the threshold in the figure corresponds to the $P < 0.005$ (uncorrected) threshold described in the text. Right in the presented images corresponds to the right hemisphere.